J. Electrochem. Sci. Eng. **14(4)** (2024) 459-472; http://dx.doi.org/10.5599/jese.2324

Open Access : : ISSN 1847-9286
https://pub.iapchem.org/ojs/index.php/JESE

Review paper

Behaviour of thermally sprayed coating for hot corrosion applications

Md Sarfaraz Alam[1,✉], Naveen Kumar[2] and Anil Kumar Das[3]

[1]*Department of Mechanical Engineering, Sershah Engineering College Sasaram, Bihar 821113, India*
[2]*Department of Mechanical Engineering, United College of Engineering & Research, Prayagraj, Uttar Pradesh (211010), India*
[3]*Department of Mechanical Engineering, National Institute of Technology Patna, Bihar 800005, India*

Corresponding authors: ✉ *mda.phd19.me@nitp.ac.In*

Received: March 16, 2024; Accepted: April 24, 2024; Published: June 16, 2024

Abstract

As modern air engines' working temperatures are increasing, materials and coatings' hot corrosion resistance characteristics gain significant attention. Hot corrosion is a type of degradation at high temperatures that involves oxidizing or sulphidation of the substrate behind a layer of salt melt deposit, which either causes the development of a thick layer of sulphide scale or the penetration of sulphur via grain boundaries into the matrix to a deeper depth. It may notably change the microstructure, phase composition, and characteristics of the thermally sprayed coating. In recent years, thermally sprayed cermet coatings on steel have been more well-liked as a possible method for enhancing hot corrosion resistance. This review paper qualitatively summarizes the recent development of thermal sprayed coatings to improve hot corrosion performance.

Keywords

Sulphidation; tribology; wear resistance; cermet coatings

Introduction

Hot corrosion is a type of degradation at high temperatures that involves oxidizing or sulfidation of the substrate behind a layer of salt melt deposit, which either causes the development of a thick layer of sulphide scale or the penetration of sulphur via grain boundaries into the matrix to a deeper depth. The typical morphology of hot corrosion products consists of a low-chromium metal matrix, a dense, porous oxide layer, and chromium-rich sulphides inside the oxides. The consensus among specialists is that initiating a hot-corrosion attack requires liquid Na sulphate. Generally, hot corrosion attack occurs between 800 and 950 °C, though this varies depending on the alloy.

If the melting point for salt deposits is at a lower temperature but the dew point is at higher temperatures, the corrosion is referred to as type I hot corrosion [1]. On the other hand, type II hot

corrosion happens at lower temperatures (generally from 670 to 750 °C). Type II hot corrosion behind a protective layer with minimal to no interior attack indicates a pitting attack [2].

Some metals, such as zirconium, titanium, chromium, and others, form shielding nitride scales when exposed to nitrogen-rich environments. Carburization and decarburization problems that weaken or embrittle the component occasionally occur in carbon dioxide and carbon monoxide environments.

When fireside boiler tubes in coal-fired steam-generating plants started to deteriorate, high-temperature corrosion was first identified as a severe issue in the 1940s. Since then, fluidized bed combustion, gas turbines, I. C. engines, boilers, and industrial waste incinerators have all experienced the issue. In the late 1960s, turbine makers and users learned about hot corrosion due to the severe corrosive assault that occurred in the engines of rescue planes and helicopters operating over and near seawater during the Vietnam War [3,4]. The primary factor contributing to hot corrosion is the breakdown of ash and fuel compounds, which include Na, S, V and Cl, which are present in burning coal or fuel oil. When marine atmospheres are contaminated with NaCl, these pollutants may occasionally be consumed from the service environment. It is well acknowledged that hot corrosion requires condensed alkali metal salts, especially Na_2SO_4 [5]. A typical high-temperature corrosion promoter in these applications, besides Na_2SO_4, is V_2O_5.

In most cases, using these low-grade fuels is acceptable due to the significant expense of eliminating these contaminants. According to research, the most frequent salt buildup in boiler superheaters is sodium vanadyl vanadate ($Na_2O \times V_2O_4 \times 5V_2O_5$), which fuses at a comparably lesser temperature of 550 °C [6]. Na_2SO_4, V_2O_5, and $Na_2V_2O_6$ are also anticipated to be the main species in salt deposits accumulating on gas turbine surfaces [7].

Due to molten salts in the fuel, such as KCl, $NaVO_3$, Na_2SO_4, V_2O_5, and NaCl, hot corrosion is the primary cause of failure in gas turbines [8-11]. This corrosion causes surface spalling by accelerating the oxidation and sulphidation of thermo-resistant materials. When contaminants like sulphur and/or chlorine are present in an oxidizing atmosphere, the rate of attack frequently increases in the sequence as first oxidation only, after that internal sulphidation, then after internal chlorination, then (sulphate salts) hot corrosion then (sulphate and chloride salts) hot corrosion. To compare other, more aggressive kinds of corrosion, oxidation in air or O_2 is typically employed as a baseline. Molten salt deposits can bring on rapid oxidation and hot corrosion. Internal chlorides, oxides, and/or internal sulphides are examples of corrosion products [12-14]. Gas turbine parts that work in the heated gas stream, such as vanes, blades and combustor cans, are exposed to severe corrosive conditions [15]. These types of corrosion can significantly reduce the lifespan of gas turbine parts. Type I hot corrosion (sulphidation and internal damage) takes place between 800 and 900 °C, whereas Type II hot corrosion (pitting) takes place between 600 and 750 °C [16]. Hot corrosion damage can be divided into two phases. First, in the incubation phase, during which the developed protective scale may be heeled by materials in the underlying substrate, metal loss rate is low. Second, in the propagation phase, during which the protective scale has been irreparably damaged, sulphides and oxides advance quickly into the surface of the substrate, and the metal loss rate is high [17].

Residual oil (fuel) is used in energy-generating systems, which is widely recognized due to the exhaustion of high-quality fuels and for financial reasons. Salt contamination from entrained brine and contaminants such as sodium, vanadium, and sulphur are present in residual fuel oil. The combustion system reacts with sodium and sulphur to produce Na_2SO_4 (melting point 884 °C). Vanadium and oxygen combine to generate the oxide V_2O_5 (melting point 670 °C) during fuel combustion. At the working temperatures of a gas turbine, V_2O_5 is a liquid in energy-generating

systems. These substances (also referred to as ash) cause rapid oxidation (also known as hot corrosion) and accumulate on the surface of the materials.

Hot corrosion is anticipated to be a concern when contemplating coal-gasification procedures since the feedstock also contains a significant quantity of salts, and the gas environment often contains sulphur and chloride compounds and low oxygen activity [18].

Gas turbines typically operate at relatively high temperatures. This trend is anticipated to continue when cooling technologies and new materials are developed for gas turbine engines of the next generation. Hot corrosion requires particular consideration due to the coupling of such elevated temperatures with an aviation condition that contains pollutants, including sodium, vanadium, sulphur, and several halides [7].

Therefore, power plants are one of the key industries affected by severe corrosion issues that cause significant losses. For example, the boiler and turbine thermal efficiency is affected by the creep and corrosion resistance of boiler and turbine elements, which limits the steam/gas temperature. The rate of power production is then lowered as a result of the decreased thermal efficiency [19].

Iron base alloys containing significant amounts of chromium and nickel are most frequently used in coal-fired power plants and oil refineries. The use of these alloys often results in their corrosion due to the attack of gaseous elements such as O_2, H_2S, SO_2, CO, and CO_2, as well as the deposition of meltable ash or salts. Numerous researchers have examined the corrosion caused by the deposit at the fireside. Alkali sulphates, which accumulate on the surface of alloy components and promote hot corrosion degradation because of less melting eutectics between $Fe_2(SO_4)_3$ and Na_2SO_4 and or K_2SO_4 or both, happen at relatively low temperatures [20-23], are the most prevalent forms of sulphates. Studies on cobalt, nickel, and Fe base alloys have shown that hot corrosion may initiate as low as 550 °C. Thus, the creation of low melting eutectics such as Na_2SO_4 + $CoSO_4$ (565 °C) and Na_2SO_4 + $NiSO_4$ (667 °C) appears to be the main cause.

Most of the time, high-temperature alloys subjected to corrosion displayed oxidation and sulphidation degradation. Type II hot corrosion is uncommon in aero engines since the blades are often operated at higher temperatures [24]. On the other hand, industrial and marine gas turbines operating at low temperatures may experience type II high-temperature corrosion at moderate temperatures.

High-temperature corrosion occurs when molten salt is applied to alloys and metals. In boilers that burn coal, corrosion arises at high temperatures due to low-emission combustion and low-quality fuel. When low-quality fuels burn, they release ash due to the presence of sulphur, salt, vanadium, chlorine, and other contaminants. On boiler parts, fly ash may create a layer of molten salt. Severe high-temperature corrosion is caused by the complex salt deposit's attack on the developed protective oxide scale of the material [25-28].

Research progress in hot corrosion

Guo *et al.* [29] deposited an Al and Cr gradient NiCoCrAlYSiB coatings on to Ni based superalloy substrate and oxidised them at 900 °C for 20 hours in 0.5 mg cm^{-2} of 20 % K_2SO_4 80 % Na_2SO_4 salt mixture to examine the effects of Al and Cr on the hot corrosion of coatings. XRD and EDS results show that there are only the alumina formed on the NiCoCrAlYSiB coatings, so the basic fluxing of Al_2O_3 occurred, which caused an accelerated hot corrosion after 10 h. The gradient coatings resulted from Al_2O_3 and Cr_2O_3 formed in the first stage of hot corrosion. Na_2SO_4's oxygen ion activity is lowered by Cr_2O_3, which reacts with Al_2O_3 more readily than Al_2O_3, protecting Al_2O_3. Similar to

oxidation kinetics, gradient coatings show hot corrosion kinetics due to the development of continuous and protective layer of Cr_2O_3 and Al_2O_3.

The hot corrosion and oxidation behaviour of the Ni and Fe-based superalloys Superni75 and Superfer 800H were investigated by Sidhu *et al.* [30]. The superalloy samples underwent cycle conditions, including exposure to air and a corrosive molten salt environment (75 % Na_2SO_4 + 25 % NaCl) at 800 °C. Superni75, a superalloy based on nickel, is more resistant to oxidation and heat corrosion than Superfer800H, a superalloy based on iron, in the given environment at 800 °C. Due to its tendency to produce protective spinel and chromium-nickel oxides, Superni 75 has performed better in both circumstances.

In a related investigation, Sidhu *et al.* [31] came to the conclusion that the oxides of the coatings' active components, which developed on the scale's surface and at the edges of Ni and W-rich splats, were responsible for the hot corrosion and resistance against oxidation of WC-NiCrFeSiB coatings. Developed oxides served as barriers to prevent the corrosive species from diffusing and penetrating through the coatings.

After being exposed to 950 °C for 20 hours, the DZ68 superalloy surface formed a protective scale, according to Liu *et al.* [32]. The procedure improved the alloy's first incubation period at 900 °C in the slurry. According to their research, it may provide a special defence against corrosive salt and dramatically slow down the rate of deterioration.

Liu *et al.* [33] examined the effects of the hot corrosion behaviours of the M38G superalloy in a combination of Na_2SO_4-NaCl salt melts. Results indicated that the treatment could, in combination with melts at 850 and 800 °C, somewhat boost the M38G alloy's resistance to hot corrosion. The protection provided by the oxide layer decreased with temperature, but the treatment at 875 °C had no effect on the hot corrosion of the M38G superalloy.

Kamal *et al.* [34] investigated the oxidation and hot corrosion behaviour of Ni-based superalloys exposed to ambient air and a corrosive fused salt environment (Na_2SO_4 - 60 % V_2O_5) at 900 °C. Weight change observation and calculation on the superalloys during the entire cycle are used to develop hot corrosion and oxidation kinetics. The enhanced hot corrosion and oxidation resistance of Superni75 was attributed to the scale's richness in NiO, Cr_2O_3, and spinel $NiCr_2O_4$. On the other hand, non-protective iron oxides and nickel and iron sulphides cause Superfer800H to have a comparatively lower level of hot corrosion resistance. The parabolic rate constants computed for these materials indicate that the hot corrosion rate for superalloys is lowest in ambient air with respect to a fused salt condition.

According to Wang *et al.* [35], The Nb solid solution / Nb_5Si_3 alloys oxidised more quickly and left the porous surface when NaCl and Na_2SO_4 were present.

According to the research of Sidhu *et al.* [36], WC-Co and WC-CoCr coatings on steel alloys T22 and T91 proved to be corrosion resistant in the boiler's superheater area after ten cycles (each lasting 100 hours) at 900 °C. The following order of coating corrosion resistance demonstrations was observed: T22 coating with 86WC-10Co4Cr > T22 coating with WC-17Co > T91 coating with WC-10Co4Cr > T91 coating with WC-17Co

The Cr_3C_2-NiCrMoNbAl coating made by HVOF on P91 steel and its hot corrosion behaviour was described by Zhou *et al.* [37]. Compared to P91 steel, the Cr_3C_2-25(NiCr) coating showed better corrosion resistance at 650 °C.

According to Qiao *et al.* [38], Nb-Si-Ti alloy and its silicide covering were subjected to a heated corrosion process that was exacerbated by NaCl.

Wei *et al.* [39] deposited the Mo-62Si-5B alloy using the SPS method. When an alloy is coated with molten salts, more significant mass changes occur compared to when exposed to dry air. The alloy's mass changes in the Na_2SO_4+NaCl combination and Na_2SO_4 following 100 hours of hot corrosion at 900 °C are 0. 50 and 0. 24 mg cm^{-2}. There is a loss of mass when SiO_2 is created because more MoO_3 evaporates than is gained in weight. Most loose oxide scales on the alloy are made up of SiO_2 and amorphous borosilicate. The oxide scales become porous due to the mixture of Na_2SO_4 and NaCl, accelerating the oxidation process.

The corrosion behaviour of WC-CoCr coatings by HVOF spraying in 0. 1 M HCl solution at 25 °C was investigated by Picas *et al.* [40] using the electrochemical polarisation method. In contrast to the steel base and thin electrolytic hard chromium coating, HVOF sprayed WC-CoCr coatings can provide better corrosion protection in the extremely corrosive 0. 1 M HCl solution.

A significant improvement in corrosion resistance to both 1 mol/L HCl and 3. 5 wt.% NaCl solutions was seen by Zhang *et al.* [41] when they investigated the corrosion characteristics of HVOF-sprayed nano-structured WC-10Co4Cr coating in two corrosive salt environments.

The hot corrosion performance of the austenitic steel weld metal was examined by Xu *et al.* [42]. It was established that the surface of the weld metal developed an outer face rich in iron and a protective layer of Cr_2O_3 after being exposed to temperatures of 700 and 800 °C for 100 hours in a fused salt environment. Yet, because the molten salt dissolves the oxide film in a 650 °C KCl-NaCl-Na_2SO_4 salt environment, significant oxidation still happens in the weld metal.

A general methodology adopted for hot corrosion includes the following steps, as shown in Figure 1. The sample is first cut to the suitable size. Before the development of the coating, the samples are prepared using sandblasting or emery paper, followed by cleaning with acetone to remove small debris. The coatings were developed by thermal spraying to the targeted substrate using prepared/available feedstock powder.

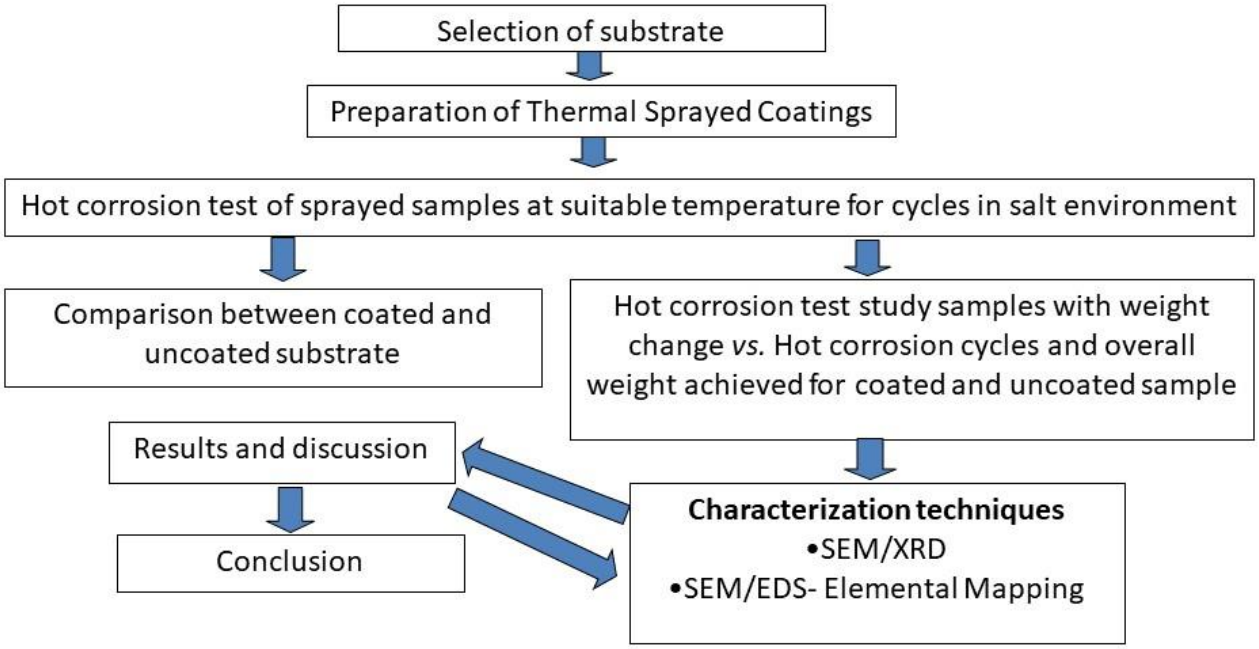

***Figure 1**. A General process flow chart for hot corrosion study*

Then, under cyclic conditions, hot-corrosion experiments were carried out in a highly corrosive salt environment of Na_2SO_4 or Na_2SO_4-NaCl or $Fe_2(SO_4)_3$ or $Fe_2(SO_4)_3$-NaCl or other corrosive salt and their combinations layered over the surface of the substrate for certain cycles. Each cycle consists

of a still-air cooling period after a high-temperature heating period around a certain temperature in a furnace. Following each hot corrosion cycle, the crucible and samples were mixed and weighed using an electronic weighing device. The spalled scales were also considered for calculating the overall corrosion rate during the weight change measurement. Surface area/weight growth was utilized to create corrosion kinetics.

X-ray diffraction analysis of the hot corroded scales

Before heat corrosion, the XRD pattern of the WC-CoCr coated surface (Figure 2) exhibits clear, sharp peaks for both WC and W_2C. The WC phase has been dissolved and decarburized, as shown by the rise in the height of the WC and W_2C peaks. The high surface area to volume ratio of feedstock powder, which made it easy for the WC atoms to interact with spraying temperature, is the primary source of decarburization in coatings [43].

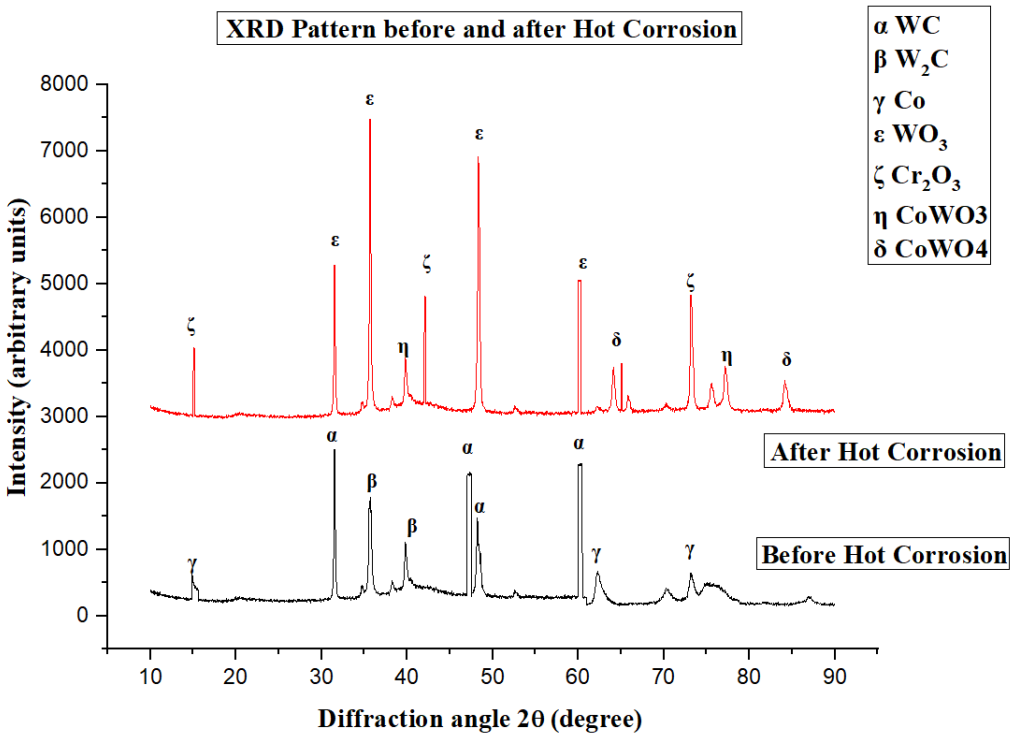

Figure 2. *XRD plot for WC-CoCr coatings and coated hot corroded scales. Reproduced from [44] with permission from Springer Nature*

Following fifty hot corrosion cycles, the XRD analysis of the WC-CoCr coated 316L steel substrate (Figure 3) revealed the formation of WO_3, CoW_3C, and $CoWO_4$ as the main phases. The intermediate phase, Cr_2O_3 and its spinel $CoCr_2O_4$, was caused by the chromium content and also contributed to the coating's ability to resist corrosion in a Na_2SO_4 25 % NaCl salt environment. Notable oxides were Fe_2O_3, $CoSO_4$, and $FeCr_2O_4$. There were also some Na traces found. A sizable number of oxide phases occurred after fifty cycles in a fused corrosive salt environment, indicating fast oxidation.

Figure 3 depicts the identified phases subjected to a salty environment $12Na_2SO_4$-$88Fe_2(SO_4)_3$ at 800 °C. XRD reveals that after hot corrosion, the specimen mainly consists of the following phases $FeSCr_2S_3$, Na_2FeO_2, $NiCr_2O_4$, and FeS phase.

A fused state of $NaFe(SO_4)_2$ is thought to develop (Equation (1)) when Na_2SO_4 and $Fe_2(SO_4)_3$ are mixed:

$$Na_2SO_4 + Fe_2(SO_4)_3 \rightarrow 2NaFe(SO_4)_2 \quad (1)$$

The Cr_2O_3 coating on the 316L steel is degraded (Equation (2)) when the alloy and this fused phase interact:

$$3Cr_2O_3 + 4NaFe(SO_4)_2 \rightarrow 2Na_2CrO_4 + 2FeS + 2Cr_2S_3 + 2Fe_2O_3 + 15O_2 \quad (2)$$

As a result, the oxide scale will be destroyed and sulphides and fluxing products will appear, as shown by Equations (3) and (4). The liquid phase further deteriorates the alloy:

$$3Fe + 2NaFe(SO_4)_2 \rightarrow 4FeS + Na_2FeO_2 + 7O_2 \quad (3)$$

$$3Ni + 2NaFe(SO_4)_2 \rightarrow 2FeS + 2NiS + Na_2NiO_2 + 7O_2 \quad (4)$$

The entire corrosion attack is controlled by the liquidus $NaFe(SO_4)_2$, and corrosion will likely be less severe because there isn't any Na_2SO_4 emission. The oxide scales on an alloy that corrodes at 800 °C are thicker than those that form at lesser temperatures. The fluxing products Na_2CrO_4, Na_2FeO_2, and Na_2NiO_2 and the development of gases cause the scales to crack or become disrupted. This causes the fused salt to contact metal and initiate a potent oxidation attack. The steel oxidizes and fluxes more quickly due to its easy oxygen availability.

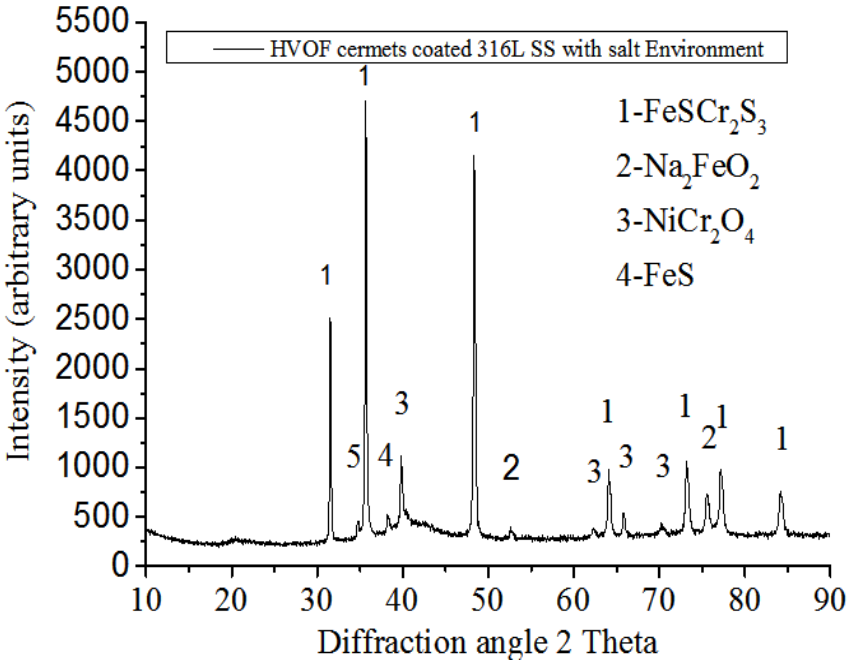

Figure 3. *XRD pattern of WC-CoCr coatings by HVOF spraying on 316L steel substrate in corrosive salt Environment. Reproduced from [45] with permission from Springer Nature*

Scanning electron microscopy analysis of the hot corroded scales

When exposed to a Na_2SO_4 + 25% NaCl salt environment, the unprotective oxide (Fe_2O_3) is generated as the surface scale of the uncoated steel substrate, allowing corrosive elements to penetrate the surface. Hot corrosion of an uncoated steel substrate results in unprotective Fe_2O_3 scales. Fe and Cl are shown as active elements in Figure 4's SEM image of the bare hot corroded sample. Fe creates an unprotective Fe_2O_3 oxide layer that is loosely retained after oxidation. Melted salt diffuses slits and cracks when it interacts with a steel substrate over 628 °C. This causes oxide scale development and oxidation to occur first.

Through the process of dissolution (Equations (5) to (10)), the fused salt paste's NaCl dissolves into Cl^- and Na^+ ions. The Cl^-ions then enter the substrate and react to form metal chlorides like $FeCl_2$ and $CrCl_2$.

$$NaCl \rightarrow Na^+ + Cl^- \quad (5)$$

$$Fe + Cl_2 \rightarrow FeCl_2 \quad (6)$$

$$4FeCl_2 + 3O_2 \rightarrow 2Fe_2O_3 + 4Cl_2 \quad (7)$$

$$2Cr_2O_3 + 8Cl^- \rightarrow 4CrCl_2 + 3O_2 \quad (8)$$

$$Na_2O + Cr_2O_3 + 1/2\ O_2 \rightarrow 2NaCrO_4 \quad (9)$$

$$4Fe + Na_2SO_4 \rightarrow 3FeO + Fes + Na_2O \quad (10)$$

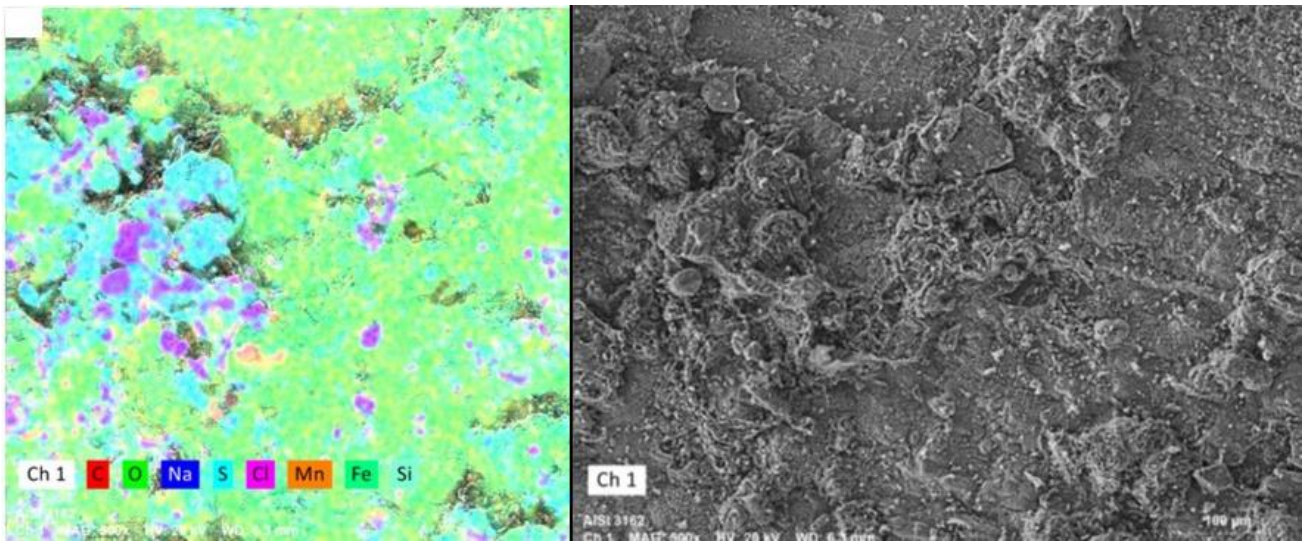

Figure 4. *SEM images of uncoated hot corroded scales. Reproduced from [44] with permission from Springer Nature*

On the top surface of the plasma sprayed WC-CoCr coated steel substrate, an adhering homogenous and continuous globular scale has formed after fifty hot corrosion cycles in a Na_2SO_4-NaCl fused salt environment (Figure 5a). Scales have largely maintained their lamellar structure throughout the investigation, as the SEM micrograph shows. Thermal stress is the cause of the microcracks that form in the scale. Open fissures expedited the entrance of corrosive materials during heating and cooling in hot corrosion cycling testing. This has made the coating's inner surface degradation more severe.

In the SEM image (Figure 5b), the scale appears to have a loose, hairy structure at higher magnifyications. The ensuing interactions between coating elements such as tungsten, cobalt, chromium, iron and the chlorine created by dissociation of NaCl result in highly volatile chlorides, which in turn cause a loose and uneven oxide scale [46]. These chlorides release chlorine when they diffuse from the scale and interact with the surrounding air oxygen.

Figure 6(a-d) shows the SEM evaluation of the cyclic corrosion of 316L steel, both bare and sprayed, in settings with 12 % Na_2SO_4-88 % $Fe_2(SO_4)_3$. The surface of the nude specimen is rather uneven. As demonstrated in Figure 6(a) and (b), the uncoated sample is considerably comparable at higher magnification, revealing some pit and fracture patterns. The SEM analysis suggests that intergranular cracking on the oxide scale may be indicated by certain surface cracks on the scale. Fe_2O_3 may form since oxygen and iron are found in significant concentrations throughout the scale's composition. There are also trace amounts of Mn, Cr, and Co.

SEM image of the hot corroded HVOF WC-CoCr 316L steel at high magnification (Figure 6(c,d)) reveals some visible globules and some unmelted powder.

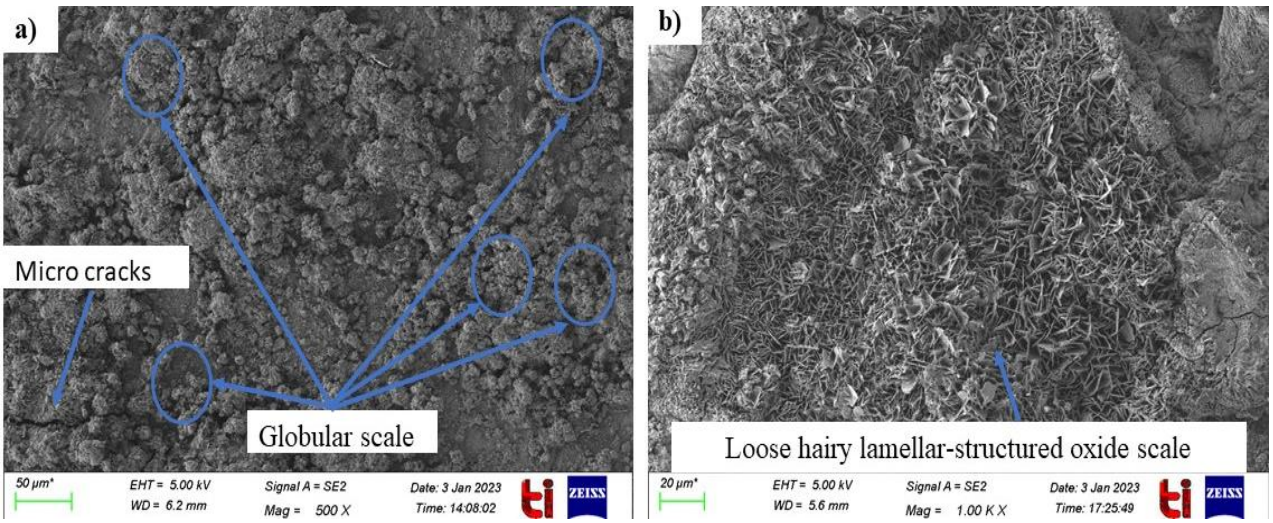

Figure 5. *SEM images of WC-CoCr coated hot corroded scales. Reproduced from Ref. [44] with permission from Springer Nature*

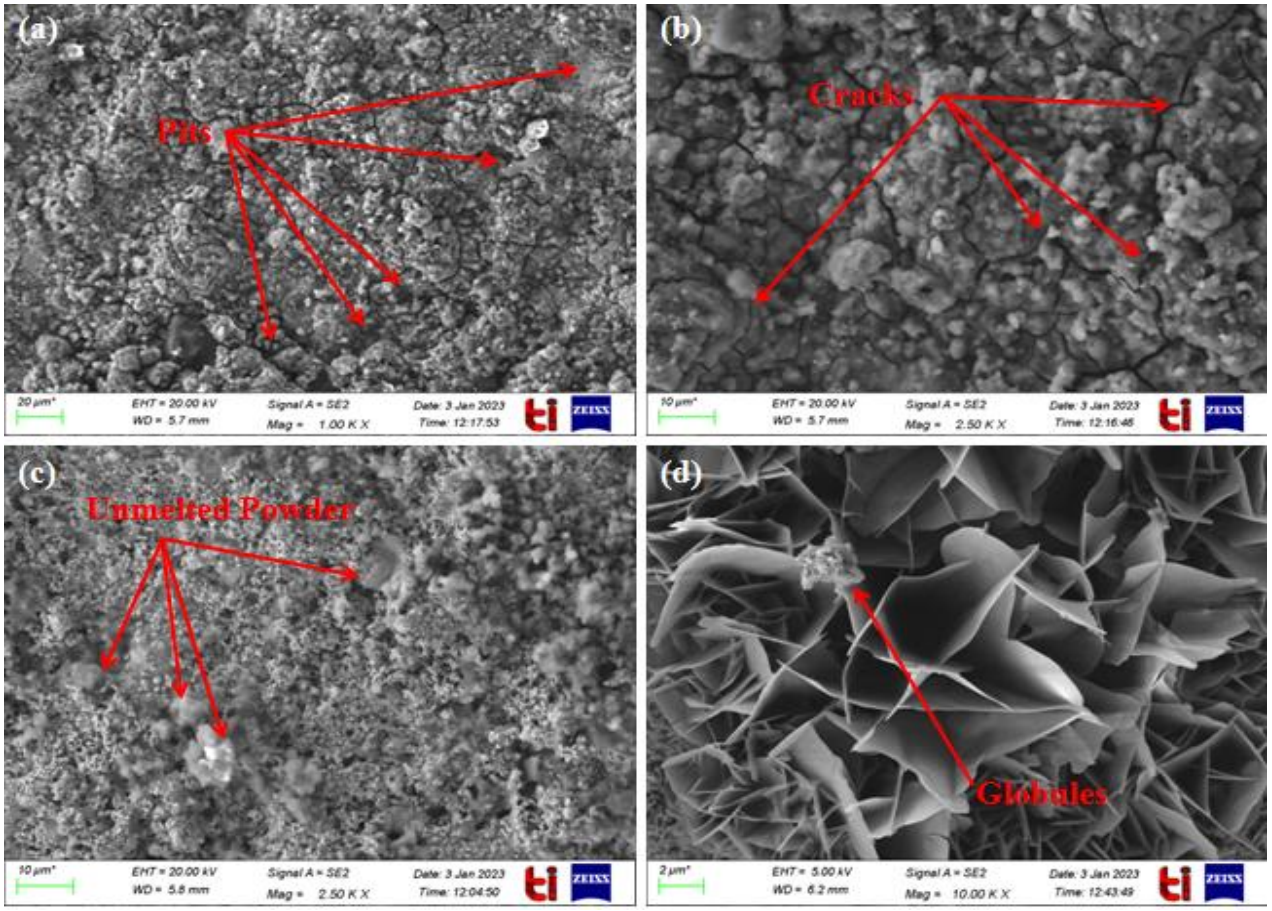

Figure 6. *SEM images (a-b) bare 316L steel (c-d) HVOF sprayed 316L steel in the corrosive salt environment at 800 °C. Reproduced from [45] with permission from Springer Nature*

The cross-sectional SEM images of the coated and bare samples following the hot corrosion test are displayed in Figure 7 (a) and (b). Figure 7(a) displays the surface for spalling and corrosion pits on bare samples when the magnification is increased [47]. Figure 7(b) shows the coated, hot-corroded sample's surface separation and microholes. This is the consequence of high-speed melt and semi-fused particles crossing over the substrate [48].

Some findings have been highlighted in Table 1

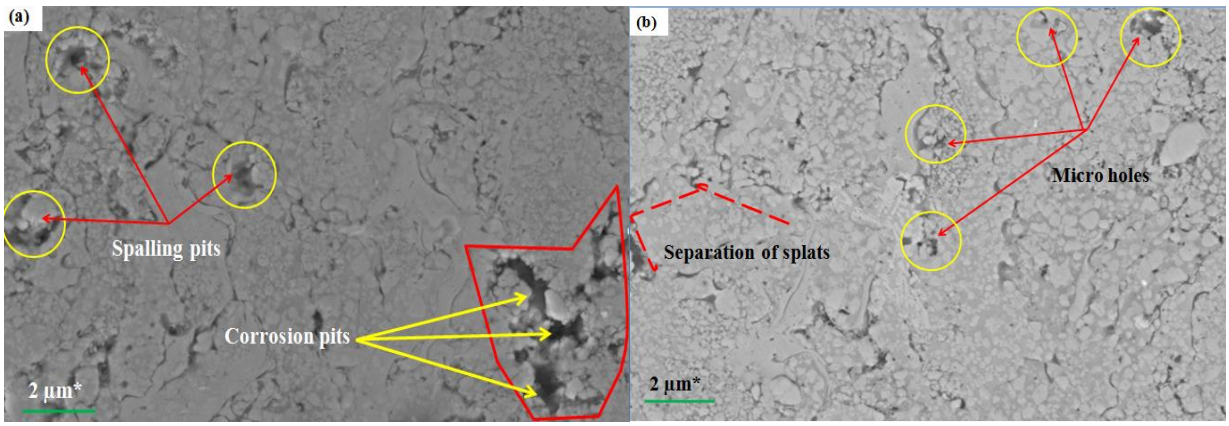

Figure 7. SEM image of cross-section (a) bare hot specimen (b) coated hot corroded specimen after hot corrosion. Reproduced from [45] with permission from Springer Nature

Table 1. *Comparative findings of coating characteristics on steel substrates*

Authors	Coating methods	Substrate	Coating powders	Findings
Alam *et al.* [44]	Plasma spray	AISI 316l	WC-Co-Cr	A significant rise in hot corrosion resistance.
Kumar *et al.* [48]	HVOF	AISI 1010	WC-Co and WC-Co-Cr	Oxidation and corrosion properties enhanced.
Alam *et al.* [49]	TIG	Carbon steel	WC, TiN and TiC,	Wear, corrosion and micro-hardness properties increased.
Hodgkiess *et al.* [50]	HVOF	Austenitic grade steel	Ni-Cr-Si-B-C	Corrosion and erosion characteristics enhanced.
De Souza and Neville [51]	D-Gun	UNS S31603 and UNS S32760	WC-Co-Cr	At liquid-solid impingement, good wear and corrosion resistance was attained.
Kumar *et al.* [52]	HVOF	SAE213 T22 and SA516Grade 70	Nano-structured Ni-20Cr	Increased resistance against erosion and corrosion in real boiler settings.
Hemmati *et al.* [53]	HVOF	carbon steel	Cr_3C_2-25NiCr	The findings demonstrated that the cladding was substantial enough to delay the onset and propagation of cracks.
Thi *et al.* [54]	APS	AISI 304	Cr_3C_2-25NiCr	Outperformed unprotected coating and sealed by traditional impregnation technique in terms of wear and corrosion resistance.
Xie *et al.* [55]	HVAF	AISI 316L	AlFeNiCoCr	Both corrosion and abrasion resistance are superior in the coating compared to the 316L stainless steel substrate.
Li *et al.* [56]	Plasma spray	38CrMoAl	Ni-Cr-Cr_3C_2	The coating's superior corrosion resistance performance is attributed to its substrate and plasma spraying technique, which enables the coating to accomplish metallurgical bonding and a more dense microstructure with high bonding strength, reduced porosity, and fewer cracks.
Jiang *et al.* [57]	Plasma spray	T91 steel	Fe-based amorphous coatings	Tested how the coating would react to heat (700 °C) in hot Na_2SO_4+K_2SO_4 salts. Due in part to the development of protective oxides of chromium and nickel, such as Cr_2O_3, NiO and $NiCr_2O_4$, the amorphous composite micro-structure and high Cr and Ni elemental concentrations produced the maximum hot corrosion resistance.
Zavareh *et al.* [58]	Plasma spray	Carbon steel	Al_2O_3-40TiO_2	The Al_2O_3-TiO_2 chemical composite that was created by the plasma spray method has better chemical and mechanical qualities.
Kannan *et al.* [59]	Plasma spray	Co-Cr-WC alloy(Stellite-21)	AZ91D-Mg alloy (Al-Zn-Mn)	When exposed to an environment that contains a coating of chloride on the binding metals, the AZ91D-Mg alloy covered with stellite cannot provide superior corrosion protection.

Summary and outlook

This article examines the most recent research and breakthroughs in the field of hot corrosion performance of various coatings. The coatings on the substrate exhibited greater hot corrosion resistance due to the protective WO_3/Cr_2O_3, etc. phases. The developed phases serve as a mechanism of transportation across this scale. These are typically slow growth in nature. Thus, an oxide retards/prevents the inward diffusion of gaseous/vapour impurities and the outward diffusion of other alloy elements.

References

[1] J. Stringer, Performance limitations in electric power generating systems imposed by high temperature corrosion, *High Temperature Technology* **3(3)** (1985) 119-141. https://doi.org/10.1080/02619180.1985.11753292

[2] J. Stringer, Coatings in the electricity supply industry: past, present, and opportunities for the future, *Surface and Coatings Technology* **108-109** (1998) 1-9. https://doi.org/10.1016/S0257-8972(98)00642-2

[3] A. R. Rapp, Y. S. Zhang. Hot corrosion of materials: fundamental studies. *JOM* **46** (1994) 47-55. https://doi.org/10.1007/BF03222665

[4] A. R. Rapp, Hot corrosion of materials: a fluxing mechanism?, *Corrosion Science* **44(2)** (2002) 209-221. http://dx.doi.org/10.1016/S0010-938X(01)00057-9

[5] T. S. Sidhu, A. Malik, S. Prakash, R. D. Agrawal, Oxidation and hot corrosion resistance of HVOF WC-NiCrFeSiB coating on Ni-and Fe-based superalloys at 800 C, *Journal of Thermal Spray Technology* **16** (2007) 844-849. https://doi.org/10.1007/s11666-007-9106-8

[6] N. Kumar, V. K. Choubey, Investigation of microstructure and Isothermal oxidation resistance of cermet HVOF coated on AISI316L at 900 °C, *Results in Surfaces and Interfaces* **14** (2024) 100173. https://doi.org/10.1016/j.rsurfi.2023.100173

[7] K. L. Luthra, and H. S. Spacil, Impurity deposits in gas turbines from fuels containing sodium and vanadium, *Journal of the electrochemical society* **129(3)** (1982) 649. https://doi.org/10.1149/1.2123941

[8] S. P. Zhu, H. Z. Huang, W. Peng, H. K. Wang, S. Mahadevan, Probabilistic physics of failure-based framework for fatigue life prediction of aircraft gas turbine discs under uncertainty, *Reliability Engineering & System Safety* **146** (2016) 1-12. https://doi.org/10.1016/j.ress.2015.10.002

[9] B. Salehnasab, E. Poursaeidi, S. A. Mortazavi, G. H. Farokhian, Hot corrosion failure in the first stage nozzle of a gas turbine engine, *Engineering Failure Analysis* **60** (2016) 316-325. https://doi.org/10.1016/j.engfailanal.2015.11.057

[10] S. Madhavan, Rajeev Jain, C. Sujatha, A. S. Sekhar, Vibration based damage detection of rotor blades in a gas turbine engine, *Engineering Failure Analysis* **46** (2014) 26-39. https://doi.org/10.1016/j.engfailanal.2014.07.021

[11] D. Pradhan, G. S. Mahobia, K. Chattopadhyay, V. Singh, Effect of surface roughness on corrosion behavior of the superalloy IN718 in simulated marine environment, *Journal of Alloys and Compounds* **740** (2018) 250-263. https://doi.org/10.1016/j jallcom.2018.01.042

[12] D. J. Baxter, K. Natesan, Breakdown of chromium oxide scales in sulfur-containing environments at elevated temperatures, *Oxidation of metals* **31** (1989) 305-323. https://doi.org/10.1007/BF00846691

[13] B. A. Gordon, V. Nagarajan, Preliminary observations of the thermodynamic predictions of Fe-Cr-Ni alloys in coal gasifier environments, *Oxidation of Metals* **13** (1979) 197-202. https://doi.org/10.1007/BF00611979

[14] M. F. Stroosnijder, W. J. Quadakkers, Review of high temperature corrosion of metals and alloys in sulphidizing/oxidizing environments II. Corrosion of alloys, *High Temperature Technology* **4(3)** (1986) 141-151. https://doi.org/10.1080/02619180.1986.11753329
[15] N. Eliaz, G. Shemesh, R. M. Latanision, Hot corrosion in gas turbine components, *Engineering failure analysis* **9(1)** (2002) 31-43. https://doi.org/10.1016/S1350-6307(00)00035-2
[16] N. Kumar, V. K. Choubey, Recent trends in coating processes on various AISI steel substrates, *Journal of Materials Science* **59(2)** (2024) 395-422. https://doi.org/10.1007/s10853-023-09239-z
[17] F. Pettit, Hot corrosion of metals and alloys, *Oxidation of Metals* **76** (2011) 1-21. https://doi.org/10.1007/s11085-011-9254-6
[18] M. M. Barbooti,, S. H. Al-Madfai, H. J. Nassouri, Thermochemical studies on hot ash corrosion of stainless steel 304 and inhibition by magnesium sulphate, *Thermochimica acta* **126** (1988) 43-49. https://doi.org/10.1016/0040-6031(88)87248-4
[19] K. Natesan, Corrosion-erosion behavior of materials in a coal-gasificationenvironment, *Corrosion* **32(9**) (1976) 364-370. https://doi.org/10.5006/0010-9312-32.9.364
[20] J. Congleton, W. Zheng, H. Hua, Stress corrosion cracking of annealed type 316 stainless steel in high-temperature water, *Corrosion* **46(8)** (1990) 621-627. https://doi.org/10.1016/0010-938X(85)90010-1
[21] A. Hendry, D. J. Lees, Corrosion of austenitic steels in molten sulphate deposits, *Corrosion Science* **20(3)** (1980) 383-404. https://doi.org/10.1016/0010-938X(80)90007-4
[22] N. Kumar, V. K. Choubey, Comparative evaluation of oxidation resistance of detonation gun-sprayed Al_2O_3-40% TiO_2 coating on nickel-based superalloys at 800 °C and 900 °C, *High Temperature Corrosion of Materials* **99(5)** (2023) 359-373. https://doi.org/10.1007/s11085-023-10157-3
[23] N. Kumar, V. K. Choubey, Experimental investigation on hot corrosion, oxidation and microstructure of WC based cermet HVOF coating, *High Temperature Corrosion of Materials* **101** (2023) 413-432. https://doi.org/10.1007/s11085-023-10179-x
[24] A. K. Koul, J. P. Immarigeon, R. V. Dainty, P. C. Patnaik, *Degradation of high performance aero-engine turbine blades,* in *Advanced materials and coatings for combustion turbines*, V. P. Swaminathan, N. S. Cheruvu, Eds., ASM International, Materials Park, OH, USA, 1994, p. 69-74. ISBN 9780871704870. https://books.google.co.in/books?id=19NSAAAAMAAJ
[25] N. K. Mishra, N. Kumar, S. B. Mishra, Hot Corrosion Behaviour of Detonation Gun Sprayed Al_2O_3-40TiO_2 Coating on Nickel Based Superalloys at 900° C. *Indian Journal of Materials Science* **2014** (2014). https://doi.org/10.1155/2014/453607
[26] T. S. Sidhu, S. Prakash, R. D. Agrawal, Hot corrosion and performance of nickel-based coatings, *Current Science* **90(1)** (2006) 41-47. https://www.jstor.org/stable/24089016
[27] S. Topolska, Santina J. Labanowski, Corrosion of evaporator tubes in low emission steam boilers, *Archives of Materials Science and Engineering* **42(2)** (2010) 85-92. http://www.amse.acmsse.h2.pl/vol42_2/4223.pdf
[28] S. Ishigai, *Steam power engineering: Thermal and hydraulic design principles*, Cambridge University Press, 1999. ISBN 9780521135184
[29] M. H. Guo, Q. M. Wang, P. L. Ke, J. Gong, C. Sun, R. F. Huang, L. S. Wen, The preparation and hot corrosion resistance of gradient NiCoCrAlYSiB coatings, *Surface and Coatings Technology* **200(12-13)** (2006) 3942-3949. https://doi.org/10.1016/j.surfcoat.2004.12.005
[30] T. S. Sidhu, S. Prakash, R. D. Agrawal, Hot corrosion studies of HVOF NiCrBSi and Stellite-6 coatings on a Ni-based superalloy in an actual industrial environment of a coal fired boiler, *Surface and Coatings Technology* **201(3-4)** (2006) 1602-1612. https://doi.org/10.1016/j.surfcoat.2006.02.047

[31] T. S. Sidhu, A. Malik, S. Prakash, R. D. Agrawal, Oxidation and hot corrosion resistance of HVOF WC-NiCrFeSiB coating on Ni-and Fe-based superalloys at 800 C, *Journal of Thermal Spray Technology* **16** (2007) 844-849. https://doi.org/10.1007/s11666-007-9106-8

[32] G. M. Liu, F. Yu, J. H. Tian, J. H. Ma, Influence of pre-oxidation on the hot corrosion of M38G superalloy in the mixture of Na_2SO_4-NaCl melts, *Materials Science and Engineering A* **496(1-2)** (2008) 40-44. https://doi.org/10.1016/j. msea. 2008. 04. 046

[33] E. Liu, Z. Zheng, X. Guan, J. Tong, L. Ning, Y. Yu, Influence of Pre-oxidation on the Hot Corrosion of DZ68 Superalloy in the Mixture of Na_2SO_4-NaCl, *Journal of Materials Science & Technology* **26(10)** (2010) 895-899. https://doi.org/10.1016/S1005-0302(10)60143-0

[34] S. Kamal, R. Jayaganthan, S. Prakash, High temperature cyclic oxidation and hot corrosion behaviours of superalloys at 900 C, *Bulletin of Materials Science* **33** (2010) 299-306. https://doi.org/10.1007/s12034-010-0046-4

[35] W. Wang, C. Zhou, Hot corrosion behaviour of Nbss/Nb5Si3 in situ composites in the mixture of Na_2SO_4 and NaCl melts, *Corrosion science* **74** (2013) 345-352. https://doi.org/10.1016/j.corsci.2013.04.057

[36] V. P. S. Sidhu, K. Goyal, R. Goyal, Comparative evaluation of hot corrosion resistance of 83WC-17CO and 86WC-10CO-4Cr coatings on some boiler steels in actual boiler in thermal power plant, *Metallography, Microstructure, and Analysis* **6** (2017) 512-518. https://doi.org/10.1007/s13632-017-0392-3

[37] W. Zhou, K. Zhou, C. Deng, K. Zeng, Y. Li, Hot corrosion behaviour of HVOF-sprayed Cr3C2-NiCrMoNbAl coating, *Surface and Coatings Technology* **309** (2017) 849-859. https://doi.org/10.1016/j.surfcoat.2016. 10.076

[38] Y. Qiao, J. Kong, X. Guo, Hot corrosion phenomena of Nb-Ti-Si based alloy and its silicide coating induced by different corrosive environments at 900° C, *Ceramics International* **44(7)** (2018) 7978-7990. https://doi.org/10.1016/j.ceramint.2018.01.238

[39] L. Wei, W. Shao, M. Li, C. Zhou, Hot corrosion behaviour of Mo-62Si-5B (at.%) alloy in different molten salts at 900 °C, *Corrosion Science* **158** (2019) 108099. https://doi.org/10.1016/j.corsci.2019.108099

[40] J. A. Picas, M. Punset, E. Rupérez, S. Menargues, E. Martin, M. T. Baile, Corrosion mechanism of HVOF thermal sprayed WC-CoCr coatings in acidic chloride media, *Surface and Coatings Technology* **371** (2019) 378-388. https://doi.org/10.1016/j.surfcoat.2018.10.025

[41] Y. Zhang, S. Hong, J. Lin, Y. Zheng, Influence of ultrasonic excitation sealing on the corrosion resistance of HVOF-sprayed nano-structured WC-CoCr coatings under different corrosive environments, *Coatings* **9(11)** (2019) 724. https://doi.org/10.3390/coatings9110724

[42] Z. Xu, W. Jinchu, Y. Zonghui, Z. Hui, P. Cong, C. Yajie, L. Xiaoquan, Hot Corrosion Behavior of Fe-Cr-Ni-Based Austenitic Heat-Resistant Steel Weld Metal in Na_2SO_4-NaCl Molten Salts at Different Temperatures, *HighTemperature Corrosion of Materials* **99(1)** (2023) 117-132. https://doi.org/10.1007/s11085-022-10144-0

[43] Y. S. Hwang, D. B. Lee, High-Temperature Oxidation of WC-20%TiC-10%Co Carbides, *Advanced Materials Research* **811** (2013) 93-97. https://doi.org/10.4028/www.scientific.net/AMR.811.93

[44] M. S. Alam, A. K. Das, Hot corrosion behavior of plasma-sprayed WC-CoCr coatings on AISI 316L steel substrate in Na_2SO_4-25% NaCl salt environment, *High Temperature Corrosion of Materials* **99(5)** (2023) 415-430. https://doi.org/10.1007/s11085-023-10162-6

[45] N. Kumar, M. S. Alam, V. Mishra, H. Vasudev, P. C. Yadav, V. K. Choubey, A comparative investigation of the effects of temperature on the oxidation resistance of high-velocity oxy-fuel coating on AISI316L, *Physica Scripta* **99** (2024) 055031. 10.1088/1402-4896/ad3c7a

[46] I. Gurrappa, Hot Corrosion Behavior of CM 247 LC Alloy in Na_2SO_4 and NaCl Environments, *Oxidation of Metals* **51** (1999) 353-382 https://doi.org/10.1023/A:1018831025272

[47] C. W. Lee, J. H. Han, J. Yoon, M. C. Shin, S. I. Kwun, A study on powder mixing for high fracture toughness and wear resistance of WC-Co-Cr coatings sprayed by HVOF, *Surface and Coatings Technology* **204** (2010) 2223-2229. https://doi.org/10.1016/j.surfcoat.2009.12.014
[48] N. Kumar, V. K. Choubey, Effect of WC-Co and 86WC-10Co-4Cr coatings on type-II hot corrosion behaviour & microstructure characteristics at 650 degree celsius, *Surface and Coatings Technology* **469** (2023) 129812. https://doi.org/10.1016/j.surfcoat.2023.129812
[49] M. S. Alam, A. K. Das, Advancement in cermet based coating on steel substrate, *Materials Today: Proceedings* **56** (2022) 805-810.https://doi.org/10.1016/j.matpr.2022.02.260
[50] T. Hodgkiess, A. Neville, S. Shrestha, Electrochemical and mechanical interactions during erosion-corrosion of a high-velocity oxy-fuel coating and a stainless steel, *Wear* **233** (1999) 623-634. https://doi.org/10.1016/S0043-1648(99)00246-X
[51] V. A. de Souza, A Neville, Corrosion and erosion damage mechanisms during erosion-corrosion of WC-Co-Cr cermet coatings, *Wear* **255(1-6)** (2003) 146-156. https://doi.org/10.1016/S0043-1648(03)00210-2
[52] M. Kumar, H. Singh, N. Singh, Fire side erosion-corrosion protection of boiler tubes by nano-structured coatings, *Materials and Corrosion* **66(7)** (2015) 695-709. https://doi.org/10.1002/maco.201407954
[53] A. R. Hemmati, S. M. Soltanieh, S. M. Masoudpanah, On the interaction between erosion and corrosion in chromium carbide coating, *Journal of Bio-and Tribo-Corrosion* **4** (2018) 10. https://doi.org/10.1007/s40735-018-0128-1
[54] H. P. Thi, T. N. Van, T. A. Nguyen, L. P. Thi, T. D. Bich, C. L. Quoc, Cr_3C_2-25NiCr cermet coating: Preparation, PTFE sealant, wear and corrosion resistances, *Journal of Thermal Spray Technology* **30** (2021) 716-724. https://doi.org/10.1007/s11666-021-01155-5
[55] X. Xie, B. Yin, F. Yin, X. Ouyang, X. Ouyang, Corrosion behavior of FeB-30 wt. % Al0. 25FeNiCoCr cermet coating in liquid zinc, *Coatings* **11(6)** (2021) 622. https://doi.org/10.3390/coatings11060622
[56] S. Q Li, Q. L. Li, S. L. Gong, C. Wang, Researching for corrosion-resistance performance of laser-hybrid plasma spraying NiCr-Cr3C2 coating, *Physics Procedia* **18** (2011) 211-215. https://doi.org/10.1016/j.phpro.2011.06.083
[57] C. Jiang, W. Liu, G. Wang, Y. Chen, Y. Xing, C. Zhang, M. Dargusch, The corrosion behaviours of plasma-sprayed Fe-based amorphous coatings, *Surface Engineering* **34(8)** (2018) 634-639. https://doi.org/10.1080/02670844.2017.1319647
[58] M. A. Zavareh, A. A. D. M. Sarhan, B. B. A. Razak, W. J. Basirun, Plasma thermal spray of ceramic oxide coating on carbon steel with enhanced wear and corrosion resistance for oil and gas applications, *Ceramics International* **40(9)** (2014) 14267-14277. https://doi.org/10.1016/j.ceramint.2014.06.017
[59] K. Mathivanan, D. Thirumalaikumarasamy, P. Thirumal, M. Ashokkumar, Investigate the corrosion properties of stellite coated on AZ91D alloy by plasma spray technique, *Thermal Science* **26(2)** (2022) 911-920. https://doi.org/10.2298/TSCI200722209K